54-71

301676

p. 13

EFFECTS OF ATMOSPHERIC VARIATIONS
ON
ACOUSTIC SYSTEM PERFORMANCE

Robert Nation
Stephen Lang
Lockheed Sanders, Inc
Nashua, New Hampshire

Robert Olsen
U.S. Army Atmospheric Sciences Laboratory, WSMR
WSMR, New Mexico

Prasan Chintawongvanich
Physical Sciences Laboratory, NMSU
Las Cruces, New Mexico

SUMMARY

Acoustic propagation over medium to long ranges in the atmosphere is subject to many complex, interacting effects. Of particular interest at this point is modeling low frequency (less than 500 Hz) propagation for the purpose of predicting ranges and bearing accuracies at which acoustic sources can be detected. A simple means of estimating how much of the received signal power propagated directly from the source to the receiver, and how much was received by turbulent scattering was developed. The correlations between the propagation mechanism and detection thresholds, beamformer bearing estimation accuracies, and beamformer processing gain of passive acoustic signal detection systems were explored.
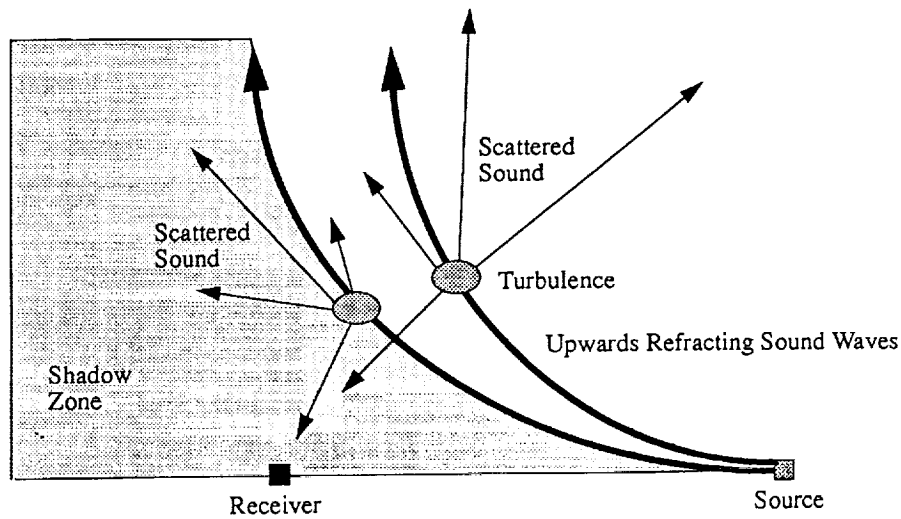
Figure 1: Upwards refraction and scattering effects on a sensor in an acoustic shadow zone.
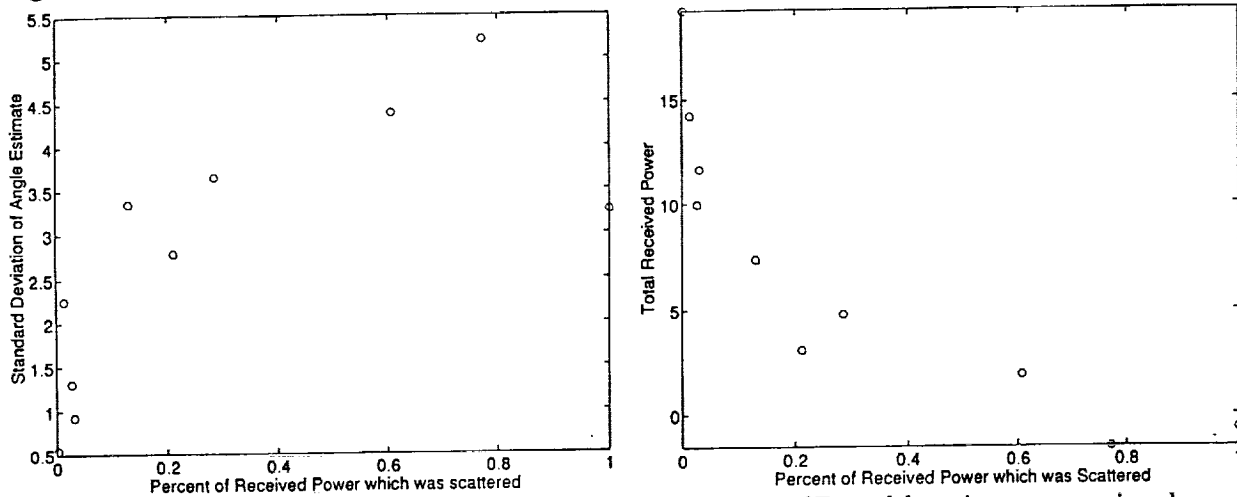

Figure 2: Received signals were attenuated by as much as 20 dB and bearing accuracies decreased by as much as 5 times when the sensor was in a shadow zone.

INTRODUCTION

Refraction and scattering together are the limiting factors in acoustic detection systems under adverse (upwards refracting) conditions, since most of the received sound is scattered (see Figure 1). Analysis of the 300 Hz tones from the short range ground to ground propagation tests at JAPE showed the sound scattered into a shadow zone was 10 to 20 dB lower in amplitude than sound which propagated directly. Bearing accuracies were reduced by as much as a factor of 5, signal detection thresholds were raised by as much as 7 dB to achieve the same probability of detection and probability of false alarm, and loss of sensor to sensor signal coherence caused as much as 2.5 dB of loss of beamforming gain when the sensor moved into a shadow zone. Figure 2 shows the effect of a shadow zone on the received signal power and bearing estimation accuracy.

IS RECEIVED POWER COHERENT OR SCATTERED?

When scattering is significant, the received signal can be modeled in the frequency domain as $S = a + b$, where a is a constant and represents the coherent, unscattered portion of the received signal, and b is the scattered component, which has had its phase randomized. b is complex normally distributed, with zero mean and variance σ_b^2. Under these conditions, the measured signal will have a Ricean distributed amplitude, or a non-central-Chi-squared distributed power.

McBride, et al [1] concluded that acoustic signals received by a sensor in a shadow zone are suitably modeled as having a Ricean distributed amplitude, where the standard deviation of the received amplitude divided by the mean is 0.52 if the signal is received entirely by scattering (in which case it is Rayleigh distributed), and the ratio decreases with an increasing directly propagating component. Alternately, we can model this as having a received power which has a non-central Chi-squared distribution, and the non-centrality factor $\lambda = 2a^2/\sigma_b^2$ increases with increasing direct propagation. λ is the amount by which the mean of the received power is increased beyond that of a central chi-squared distributed (completely scattered) signal.

The expected value of the measured power is

$$E(P) = \frac{\sigma_b^2}{2}[2 + \lambda] \tag{1}$$

and the variance of the measured power is

$$\sigma_P^2 = \frac{\sigma_b^4}{2}[2 + \lambda]\left[1 + \frac{\lambda}{2 + \lambda}\right] \tag{2}$$

We expect to observe a central Chi-squared (2 degrees of freedom) distribution for a totally scattered signal. If we chose to use the variance divided by the mean squared of the received signal as the metric of scattered-ness, then, for a completely scattered signal, the metric, r, will be 1:

$$r = \frac{\sigma_P^2}{E^2(P)} = \frac{4 + 4\lambda}{(2 + \lambda)^2} \tag{3}$$

Note that, as the direct component of the received signal increases, the non-centrality factor, λ, increases, and r approaches 0. As the scattered component increases, λ approaches 0 and r approaches 1.

We can now solve for the scattered and direct components of the received signals:

$$\hat{P}_S = \sigma_b^2 = \frac{rE(P)}{1 + \sqrt{1 - r}} \tag{4}$$

$$\hat{P}_C = E(P) - \sigma_b^2 \tag{5}$$

where $\hat{P}_S$ is the scattered component of the power, $\hat{P}_C$ is the directly propagating component, and $E(P)$ is the average received power. The percent of the received power which is scattered is $100r/(1 + \sqrt{1-r})$.

Verification with JAPE data

A suitable subset of the MIT Lincoln Laboratory's JAPE data set was identified for verification purposes. The selected tests were the ones which contained samples of ground to ground propagation of a 300 Hz sinusoid over a 500 meter distance. 300 Hz was selected because it is in the middle of the frequency range of interest, and is high enough in frequency to have a good SNR, but not so high that anti-aliasing filter concerns need to be addressed. A total of 10 such tests were identified, consisting of 5 pairs of tests in which North to South and South to North propagation was tested in rapid succession. More information about the JAPE tests can be found in [2].

Based on Equations 4 and 5 the direct and refracted component of the received power was estimated for each test. The results are shown in Table 1. By using the percent scattered power from the table, an upward/downward refraction condition decision was made, and compared to the decision made based on ray-trace plots. In 6 out of 10 cases, the decision was the same as obtained by examining ray-trace plots. The ray-trace plots were generated based on meteorological measurements. In the remaining 4 cases, the decision made based on Equations 4 and 5 better suited the received power levels than the decision made based on the ray trace plots. When looking at the revised refraction condition estimates, we note that, for all downward refracting cases, the received power was 3 dB or more. For upwards refracting conditions, the received power was 2 dB or less. This clean separation of received power levels into different classes was not obtained with decisions made based on the ray-trace plots, and gives us confidence in our separation criteria. Figure 3 plots the portion of the signal which is received by direct propagation and by scattering vs. percent scattered power, and is consistent with theory. Note that the received scattered power levels are fairly constant, regardless of refraction conditions, but that the coherent portion of the received signal decreases dramatically as upwards refraction begins to dominate. The scattered component of the received power is negligible under downwards refracting conditions.

Some possible explanations for the poor correlation between the raytrace plots and the measured acoustic data include:

- The raytraces are up to an hour different in time than the tests.

- The raytraces are apparently intended for looking at propagation over a 10-20 km range, not a 500 meter range.

- With only the raytraces, we are forced to make an upwards/downwards refracting decision, instead of percent upwards and percent downwards.

- Vertical sampling of the meteorological data near the ground may not have been adequate to accurately model conditions [3].

Table 1: Percent of Received Power which was Refracted

Test	Percent Scattered Power	Scattered Power (dB)	Coherent Power (dB)	Total Power (dB)	Refraction Condition (Note 3)	Refraction Condition (Note 4)
T005102	61	-0.3	-2.2	1.90	Up	Down
T006102	28	-0.6	3.4	4.8	Down	Down
T025102	3	-3.4	11.5	11.7	Down	Up
T026102	13	-1.5	6.8	7.4	Down	Down
T033102	21	-3.7	2.1	3.1	Down	Up
T034102	3	-5.8	9.9	10.0	Down	Down
T060102	100	-0.4	-4.9	-0.7	Up	Up
T061102	1	-4.4	14.2	14.3	Down	Down
T068102	77	-2.6	-7.9	-1.5	Up	Up
T069102	0	-7.7	19.3	19.3	Down	Up

Notes:
1. For test T060102, the percent scattered power was calculated at 114%, which was attributed to statistical variation, and rounded down to 100%.
2. Powers are measured in dB in a 0.25 Hz band relative to an arbitrary reference.
3. The refraction conditions in column 6 are derived by examining the percent scattered power. 0-50 is Down, 50-100 is Up.
4. Refraction conditions in column 7 are based on raytrace plots.
5. Results are for 300 Hz tones only.
6. Percent Scattered Power is $r/(1 + \sqrt{1 - r})$.

IMPACT OF REFRACTION CONDITION ON DETECTION THRESHOLD

If a high probability of detection (P_d = 0.90) is required coherent signals can be detected at 7 dB less signal-to-noise ratio (SNR) than incoherent, or scattered signals. Figure 4 shows the probability of detection vs SNR curves for both types of signals. The non-fluctuating case is a coherent signal, modeled as a sinusoid, and the fluctuating case is a Swerling I model [4]. The false alarm rate for the points in Figure 4 is a constant $P_f = 10^{-4}$.
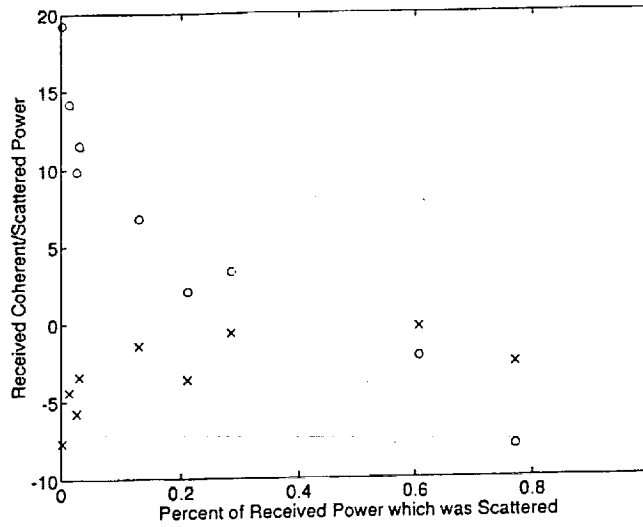
Figure 3: Scatter plot of coherent and scattered components of received power vs. percent scattered power. Coherent component is plotted with circles, and scattered component is plotted with X's. As expected, the directly propagating component increases as the percent scattered power approaches zero, and vanishes as it approaches 1. The scattered power levels are fairly constant, regardless of refraction conditions.

For low probabilities of detection, fluctuating signals are more detectable than non-fluctuating signals, since the fluctuating signal occasionally has a high SNR and is detected. Since the crossover point is about $P_d = 0.27$, this is not particularly useful.

IMPACT OF REFRACTION CONDITION ON BEARING ESTIMATION ACCURACY

Acoustic detection systems can be used as target tracking or cuing systems if they can provide a sufficiently reliable bearing estimate to the target. Bearing estimates are affected by received SNR, signal coherence, and propagation path effects. A sensor in a shadow zone, receiving primarily scattered power, experiences a loss of received SNR compared to a directly propagated signal, a loss of coherence associated with scattering, and an indirect propagation path. The combined effect for the JAPE data was a degradation in bearing accuracy of up to a factor of 5 when compared to a directly propagated signal. The loss of bearing accuracy may also result in a reduction in the system's ability to determine that two signals originated from different sources, based on their angle of arrival.

For a correlating beamformer,

$$\hat{\theta} = \max_{\theta} \left(\sum_i S_i e^{-j(\vec{k}(\theta) \cdot \vec{r}_i)} \right) \tag{6}$$

where $\vec{k}(\theta)$ is the wave vector, and $\vec{r}_i$ is the location of the sensor relative to a reference point.
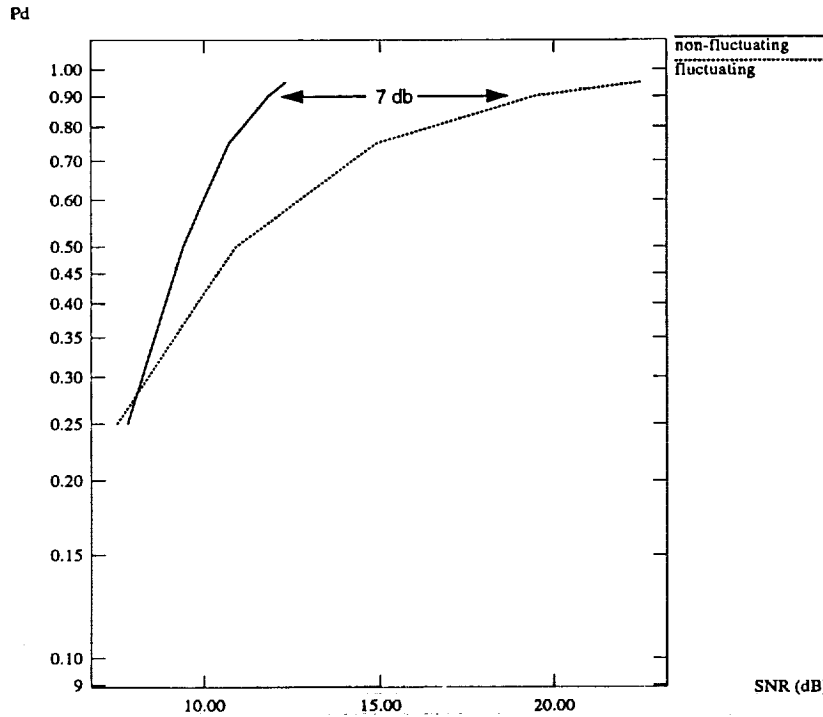
Figure 4: Coherent signals can be detected at 7 dB less SNR than incoherent signals, for $P_d = 0.9$ and $P_f = 10^{-4}$

All sensors are assumed to have the same gain. If the received power level is the same for all sensors (a valid assumption for small aperture arrays), and the array is circular, then the bearing accuracy is

$$\sigma_\theta^2 = \frac{c^2 D_s}{(N-1)(2\pi\rho f)^2} \tag{7}$$

where c is the acoustic propagation speed, D_s is the average phase structure function for all sensors, N is the number of sensors, ρ is the radius of the sensor array, and f is the signal frequency.

Daigle studied straight line propagation [5] (which we expect to be roughly descriptive of downwards refracting conditions), and determined that

$$D_S(R,\rho) = <[\phi_1 - \phi_2]^2> \approx \sqrt{\pi} < \mu^2 > k^2 R L \tag{8}$$

where $< \mu^2 >$ is the fluctuation in the acoustic index of refraction, which is written as $n = 1 + \mu$, k is the signal wave-number, R is the propagation path length, and L is correlation length. C_n^2, the acoustic index of refraction squared, is related to $< \mu^2 >$ by $C_n^2 \left| r^{2/3} \right| = < \mu^2 >$, where r is the sensor separation. C_n^2 can be computed [6] from measurements taken at JAPE via

$$C_n^2 = \frac{C_v^2}{c_o^2} + \frac{C_T^2}{4T_o^2} \tag{9}$$

47

where C_v is the speed of sound structure function, c_o is the average speed of sound, C_T is the temperature structure function, and T_o is the average temperature [7].

From the above equations, we can see that the bearing estimation error of an acoustic direction-finding system is proportional to the phase structure function of the received signal, and inversely proportional to its frequency. The phase structure function is proportional to the fluctuation in the acoustic index of refraction.

McBride, *et al.* [1, 8] show that, in an upwards refracting environment, propagation can be appropriately modeled by having upwards propagating signals scattered off of a finite number of turbules which lie in their paths. The loss of the coherent portion of the received signal under upwards refracting conditions is expected to cause bearing estimation accuracy to decrease when compared to downwards refracting conditions.

These equations neglect an important factor relating to bearing estimation: if we examine a short segment of data, during which time the refraction conditions did not change, then, at the same time that turbulence is increasing the phase structure function, and degrading bearing estimation accuracy, it is increasing the amount of energy which is scattered, and the amount of received energy, which improves bearing accuracy. The relationship between received SNR and bearing error is

$$\sigma_{\hat{\theta}}^2 = \frac{c^2}{(N-1)(2\pi f\rho)^2 SNR} \tag{10}$$

where SNR is the received signal-to-noise power ratio. The relative importance of phase perturbation and signal-to-noise ratio varies depending on signal strength.

Verification against JAPE data

Using the data presented in Table 2 we can compare the average bearing accuracy during periods of upwards refraction (4.3°) to the average bearing accuracy during periods of downwards refraction (2.2°). The expected degradation associated with upwards refraction is observed.

Figure 5 shows the relationship between C_n^2, the total received power, and the phase structure function, for a short period of time during upwards refracting conditions. Note all but one increase in the phase structure function occurred at the exact same time as a dip in the received power levels, but the relationship between C_n^2 and the received power and phase structure function is not so obvious. From this we conclude that, for this data segment, over short periods of time the bearing estimation accuracy is dominated by changes in the received power levels, not by changes in C_n^2. Note that the C_n^2 data was delayed 250 seconds to allow for the turbulence field to move

48

Table 2: Comparison of bearing estimation accuracy to other key parameters.

Test	C_n^2	Refraction	Received Acoustic Power (dB)	Received SNR (dB)	Phase Structure Function (radians^2)	σ_θ (degrees)
T005102	2.45e-6	Up	1.9	41	2.3e-1	4.4
T006102	2.45e-6	Down	4.8	42	1.6e-1	4.1
T025102	6.61e-7	Down	11.7	51	7.8e-3	0.9
T026102	1.13e-6	Down	7.4	47	1.1e-1	3.3
T033102	8.20e-7	Down	3.1	40	7.0e-2	2.8
T034102	4.43e-7	Down	10.0	50	1.5e-2	1.3
T060102	1.24e-6	Up	-0.7	37	9.7e-2	3.3
T061102	1.30e-6	Down	14.3	51	5.3e-2	2.3
T068102	2.17e-6	Up	-1.5	35	4.0e-1	5.2
T069102	2.88e-6	Down	19.3	55	1.2e-2	0.6

Notes:
1. C_n^2 measurements are 15 minute averages at 2 meter altitude.
2. Refraction is determined by computing the percent scattered power Eqs 3 through 5.
3. Powers are 30 second averages, in dB relative to an arbitrary pressure, for a 300 Hz tone.

from the meteorological measurement tower to the center of the propagation path. This delay, which assumes that the turbulence field is frozen, may contribute to the poor correlation.

For the tests examined earlier, the received SNR was between 35 and 55 dB, which induces angular errors of between 0.37 and 0.04 degrees, which was not significant compared to the measured errors. For the data in figure 5, the received signal's average SNR was only 18 dB, which causes an average bearing error of $\sigma_\theta = 2.6°$. If we examine the received power vs. time curve from Figure 5, we note that the power has drop-outs of 20 dB or more, making the received SNR during these times a mere -2dB, resulting in an expected σ_θ of 26°, and a phase structure function of about 1.6 radians^2, which is exactly what was observed. The received power on this trial was lower than on the other trials that were explored, because a set of tones was played, instead of a single tone. Since the other trials were single tones, the received SNR was higher, and the dropouts in received power levels were less significant. Unfortunately, the other tests did not last long enough to look for a short term correlation between phase structure function and C_n^2.

The results obtained from Figure 5 are significant to acoustic detector design, since average received SNRs of 18 dB are well into the detectable range for such systems. The conclusion is that the direct effect of atmospheric turbulence on the bearing accuracy of such systems can be neglected, but the indirect effect, which causes drop-outs in received power levels, and results in a decrease in angular accuracy, can not be neglected. Acoustic detectors should be designed to make bearing
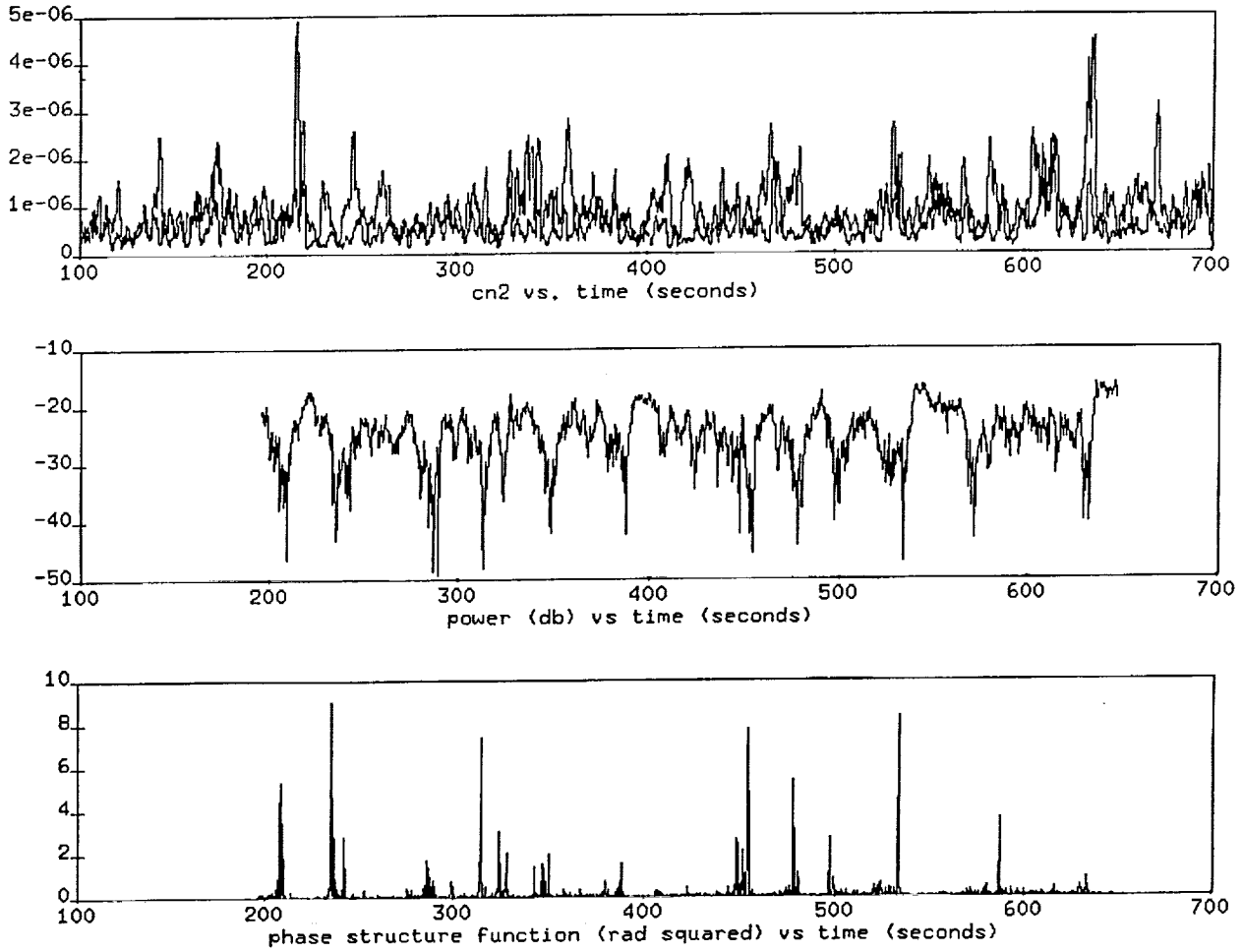
Figure 5: C_n^2 data, measured at 8 and 16 meters altitude, is delayed 250 seconds and plotted on the same scale as received power and phase structure function. Note that all but one increase in the phase structure function is matched in time to a dip in the received power. Also note that the two strongest peaks in C_n^2 match two strong increases in received power.

estimates during the peaks in the received power levels, and should avoid using the data received during the drop-outs.

Further tests to look for short-term correlation between C_n^2 and angular accuracy are needed. The tests which are missing from the JAPE data consist of playing a single, loud tone over a 500 meter propagation distance, for a long period of time (10 minutes or more). Meteorological data should be collected at a point as close to the midpoint of the propagation path as possible, and for a time covering about 10 minutes before and after the acoustic test.

IMPACT OF REFRACTION CONDITION ON BEAMFORMER PROCESSING GAIN

Beamforming gain is one of the most significant contributors to processing gain. Gain is achieved by attenuating sound from all directions but one. This attenuation is also exploited for direction finding. For perfectly correlated signals, beamforming gain is approximately

$$G = 10 \log N \tag{11}$$

where N is the number of sensors. This level of gain is achieved because target signals add coherently, so that the output power is N^2 times the input power, while noise and interference signals add incoherently, so that output power is N times the input power.

Coherence is used to measure how well signals are correlated. Coherence is defined as

$$\Gamma_{ij} = \frac{< S_i S_j >}{< S_i >< S_j >} \tag{12}$$

It can be shown that

$$\Gamma(r, \rho) = e^{-D(r,\rho)/2} = e^{-(D_X + D_S)/2} \tag{13}$$

where $D(r, \rho)$ is the signal's structure function after propagating a distance r to two sensors which are ρ apart, D_X is the amplitude structure function, and D_S is the phase structure function.

For a correlating beamformer, the loss of beamformer gain due to loss of coherence is

$$L = -10 \log \left[\frac{\sum_{ij} \Gamma_{ij}}{N^2} \right] \tag{14}$$

where N is the number of sensors, and Γ_{ij} is the coherence between sensors i and j. If we assume that all $\Gamma_{ij} = \Gamma$ if $i \neq j$ and $\Gamma_{ii} = 1$, then this reduces to

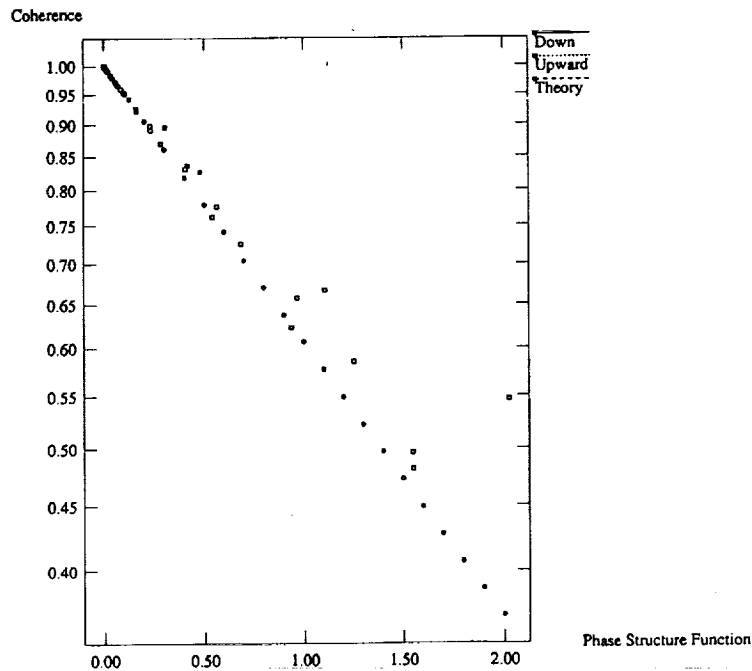$$L = -10 \log \left[\frac{1 + (N-1)\Gamma_{ave}}{N} \right] \tag{15}$$

Figure 6: An expected relationship between signal coherence and phase structure function was observed.

Verification with JAPE data

Equation 13 describes the expected relationship between the phase structure function and the coherence between the signal received on two sensors. The relationship is borne out by the data, if D_X is neglected as Daigle suggests (D_X has been shown to be smaller than D_S in practice). Figure 6 shows the relationship for upwards and downwards refracting cases, and for Equation 13.

The effect of coherence on beamformer gain has been stated in Equation 15. From Figure 6, we can see that, for downwards refracting cases, the minimum measured coherence was 0.8, which results in a loss of 0.84 dB of gain in an eight element, 1 meter radius correlating beamformer. While small, this loss is measurable. For upwards refracting cases, the smallest measured coherence was 0.5, resulting in a loss of beamformer gain of 2.5 dB, which is significant.

SUGGESTIONS FOR FUTURE WORK

Additional data collection tests would allow a more thorough investigation of some interesting phenomena:

- long duration (10 minutes or more), short range, single tone tests could be used to look for the expected short-term correlation between micro-met and acoustic data. Although we looked for this correlation, the data set was not sufficient to make a definite decision about whether or not this correlation existed.

- time-of-arrival fluctuation tests for medium and long range propagation of impulsive noises would aid in designing and evaluating acoustic ranging systems.

- tests to verify scattering model predictions, ie. bearing estimation error and frequency correlation bandwidth, under upwards refracting conditions. Existing data can be used to measure bearing estimation error, but there were not many tests performed under upwards refracting conditions.

References

[1] Walton E. McBride, Henry E. Bass, Richard Rasspet, and Kenneth E. Gilbert. Scattering of sound by atmospheric turbulence: A numerical simulation above a complex impedance boundary. *The Journal of the Acoustical Society of America*, 90(6):3314–3325, 1991.

[2] Bruce W. Kennedy, Robert Olsen, John R. Fox, Richard Savage, George Mitchler, and Richard Okrasinski. Joint acoustic propagation experiment project summary. Technical report, The Bionetics Corporation and the US Army Atmospheric Sciences Laboratory and the Physical Sciences Laboratory of the New Mexico State University, September 1991.

[3] J. S. Robertson. Numerical simulation of intensity fluctuations caused by wind gusts. *The Journal of the Acoustical Society of America*, 87(3):1353–1355, March 1990.

[4] Lamont V. Blake. *Radar Range-Performance Analysis*. Artech House, Inc., 1986.

[5] G. A. Daigle, J. E. Piercy, and T. F. W. Embleton. Propagation of sound in the presence of gradients and turbulence near the ground. *The Journal of the Acoustical Society of America*, 79(3), 1986.

[6] Edmund H. Brown and S. F. Clifford. On the attenuation of sound by turbulence. *The Journal of the Acoustical Society of America*, 64(4), October 1976.

[7] P. Chintawongvanich and Robert Olsen. Experimental study of temperature structure parameter in the surface layer. *Seventh Symposium on Meteorological Observations and Instrumentation and Special Sessions on Lower Atmospheric Studies*, January 1991.

[8] Walton E. McBride, Henry E. Bass, Richard Rasspet, and Kenneth E. Gilbert. Scattering of sound by atmospheric turbulence: Predictions in a refractive shadow zone. *The Journal of the Acoustical Society of America*, 91(3):1336–1340, 1992.